Research Square

Preprints are preliminary reports that have not undergone peer review.
They should not be considered conclusive, used to inform clinical practice,
or referenced by the media as validated information.

Cause–Effect Structure and Structural Pathways of Resilience Engineering in an Iranian Petrochemical Complex: An Integrated Fuzzy DEMATEL–MMDE–SEM Study

Reza Yeganeh
Shoushtar Faculty of Medical Sciences
Fakhradin Ghasemi
Abadan University of Medical Sciences
Arman Amiri
Shiraz University of Medical Sciences
Gholam-abbas Shirali
Ahvaz Jundishapur University of Medical Sciences
Payam Rashnoudi
P.rashnoudi@modares.ac.ir

Abadan University of Medical Sciences

Article

Keywords: Resilience Engineering, Petrochemical Industry, Fuzzy DEMATEL, Maximum Mean De-Entropy, Structural Equation Modeling, Cause–Effect Analysis

Posted Date: September 21st, 2026

DOI: https://doi.org/10.21203/rs.3.rs-10541347/v1

License: This work is licensed under a Creative Commons Attribution 4.0 International License.
Read Full License

Additional Declarations: No competing interests reported.

Cause–Effect Structure and Structural Pathways of Resilience Engineering in an Iranian Petrochemical Complex: An Integrated Fuzzy DEMATEL–MMDE–SEM Study

Reza Yeganeh[1], Fakhradin Ghasemi[2], Arman Amiri[3], Gholam-abbas Shirali[4], Payam Rashnoudi[2*]

1.Assistant professor in Occupational Health Engineering, Shoushtar Faculty of Medical Sciences, Shoushtar, Iran

2.Occupational Health and Safety Engineering Department, Abadan University of Medical Sciences, Abadan, Iran

3.Student Research Committee, Shiraz University of Medical Sciences, Shiraz, Iran

4.Department of Occupational Health Engineering, School of Public Health, Ahvaz Jundishapur University of Medical Sciences, Ahvaz, Iran

* Corresponding author. Email address: P.rashnoudi@modares.ac.ir

Abstract

Background
Resilience engineering emerges from interactions among organizational and operational capabilities, yet these interactions are rarely mapped and empirically tested within a unified analytical framework.

Methods
This study integrated fuzzy decision-making trial and evaluation laboratory (DEMATEL), maximum mean de-entropy (MMDE), and covariance-based structural equation modeling to examine 12 resilience engineering indicators in an Iranian petrochemical complex. Expert judgments from 10 specialists were used to map the influence network, and survey data from 343 employees were used to test the MMDE-retained relationships.

Results
In the expert-derived DEMATEL network, management commitment, awareness, reporting culture, learning culture, teamwork, and buffering capacity occupied net-cause positions, whereas preparedness, flexibility, self-organization, redundancy, anticipation, and fault-tolerance occupied net-effect positions. MMDE retained 10 of 132 candidate relationships. The structural model showed acceptable fit (CFI = 0.959; RMSEA = 0.027), and all 10 prespecified paths were positive and significant. Awareness showed its strongest associations with self-organization and flexibility and had significant total effects on preparedness and fault-tolerance, partly through buffering capacity and flexibility.

Conclusions
These findings distinguish overall network position from path-specific influence and provide convergent evidence that awareness and usable adaptive capacity are central to resilient performance. Given the single-site, cross-sectional design, the identified directions should be interpreted as empirically supported structural associations rather than definitive causal effects.

Keywords: Resilience Engineering; Petrochemical Industry; Fuzzy DEMATEL; Maximum Mean De-Entropy; Structural Equation Modeling; Cause–Effect Analysis

1. Introduction

The petrochemical industry plays a pivotal role in Iran's economic infrastructure, contributing substantially to national industrial development, revenue generation, and employment [1]. Given its strategic importance, ensuring operational safety and resilience in this high-risk sector is essential not only for the performance of individual plants but also for broader economic and societal stability [2] .Moreover, environmental sensitivities, sanctions, and economic fluctuations in Iran further underscore the necessity of enhancing resilience.

Traditionally, safety management in industrial systems has relied on the Safety-I approach, which assumes that adverse events result from linear, identifiable chains of failure, often attributed to human error [3–5]. This perspective emphasizes error reduction through predefined procedures and hazard elimination, assuming that system behavior can be fully predicted and controlled using past experience, risk assessments, and incident reports [6,7]. However, as industries have become increasingly complex and interconnected, such linear models have proven insufficient to capture the nonlinearity, unpredictability, and systemic interactions that characterize modern industrial environments. In high-risk domains such as petrochemical plants, traditional methods frequently fail to fully account for emerging and unforeseen threats arising from dynamic interactions among technical, human, and organizational factors [4,7–9].

Resilience Engineering (RE) has therefore emerged as a complementary systemic paradigm to address these shortcomings. Introduced in the early 2000s by Hollnagel, Woods, and other scholars in the field, RE shifts the focus from exclusively preventing failures to enhancing the system's capacity to adapt and succeed under variable conditions [10,11]. It highlights the importance of anticipating disruptions, monitoring ongoing processes, learning from both successes and failures, and responding flexibly to unexpected changes [12,13]. According to this view, a resilient system is not merely one that avoids failure, but one that continuously adapts, reorganizes, and sustains its functionality even under stress or disruption [10,11]. Resilience can be conceptualized in terms of complementary capacities that enable systems to anticipate and mitigate emerging risks, adapt to changing conditions, respond effectively to disturbances, and recover while maintaining essential functions [14,15]. These capabilities are particularly critical in volatile sectors such as petrochemical

production, where disruptions may cause severe environmental, financial, and social consequences [16,17].

Accordingly, researchers have identified measurable indicators—such as flexibility, anticipation, awareness, redundancy, self-organization, learning culture, and management commitment—that collectively represent a system's adaptive potential [16,18]. Previous studies have frequently employed multi-criteria decision-making (MCDM) techniques, including the analytic hierarchy process (AHP) and the technique for order preference by similarity to an ideal solution (TOPSIS), to rank and prioritize complex organizational and system-level factors[14,19–21]. While these methods provide useful insights into the relative importance of system-level factors, they do not explicitly reveal the direction and intensity of interdependencies among interacting resilience indicators. To address this limitation, the fuzzy Decision-Making Trial and Evaluation Laboratory (DEMATEL) method can be used to distinguish between cause and effect indicators through expert judgments and to reveal the underlying influence structure of a complex system. However, DEMATEL may generate a dense network of interrelationships, and directly translating all identified links into a structural model can lead to excessive model complexity[22–25]. The Maximum Mean De-Entropy (MMDE) algorithm provides an objective mechanism for identifying the most informative relationships and reducing reliance on subjectively selected thresholds[26]. In parallel, Structural Equation Modeling (SEM) offers a robust statistical framework for empirically testing theoretically or analytically predefined structural relationships using observed data.

To date, studies in resilience engineering have typically applied causal mapping approaches such as DEMATEL or empirical structural modeling techniques such as SEM as separate analytical strategies [22–25]. Consequently, limited evidence is available on analytical frameworks in which expert-derived cause–effect structures are systematically screened and subsequently subjected to empirical structural validation using independent field data. The integration of fuzzy DEMATEL, MMDE, and SEM addresses this methodological gap by assigning a distinct role to each analytical stage: DEMATEL identifies the cause–effect structure, MMDE extracts the critical relationships, and SEM empirically tests the resulting structural hypotheses. This sequential design enables the triangulation of expert judgments with employee survey data and provides a more rigorous basis for examining the interdependencies among resilience engineering indicators.

The aim of this study is to examine the cause–effect structure and empirically test the critical structural relationships among resilience engineering indicators in an Iranian petrochemical complex through an integrated analytical framework. First, fuzzy DEMATEL was used to identify the influence structure and classify the indicators into cause and effect groups. The MMDE algorithm was then applied to extract the most critical interrelationships and provide an objective basis for structural hypothesis development. Finally, SEM was used to empirically test the selected pathways using employee survey data. This integrated approach provides a systematic framework for linking expert-derived causal knowledge with empirical structural evidence and identifying the most influential pathways through which resilience engineering indicators interact in a high-risk process industry.

2. Materials and Methods

The overall analytical framework of the study is illustrated in Figure 1. Two complementary sources of data were used. First, expert judgments regarding the interrelationships among the twelve RE indicators were collected through pairwise comparisons. These judgments were analyzed using fuzzy DEMATEL to characterize the cause-effect structure among the indicators and classify them according to their net influence roles. MMDE was subsequently applied to the defuzzified total-relation matrix to identify the most informative relationships and provide an objective basis for structural hypothesis development. Second, employee survey data were collected using a validated resilience engineering questionnaire. SEM was then used to empirically test the predefined relationships derived from the combined DEMATEL-MMDE procedure. This sequential analytical framework enabled expert-derived system knowledge to be systematically translated into testable structural hypotheses and subsequently evaluated using independent field data.

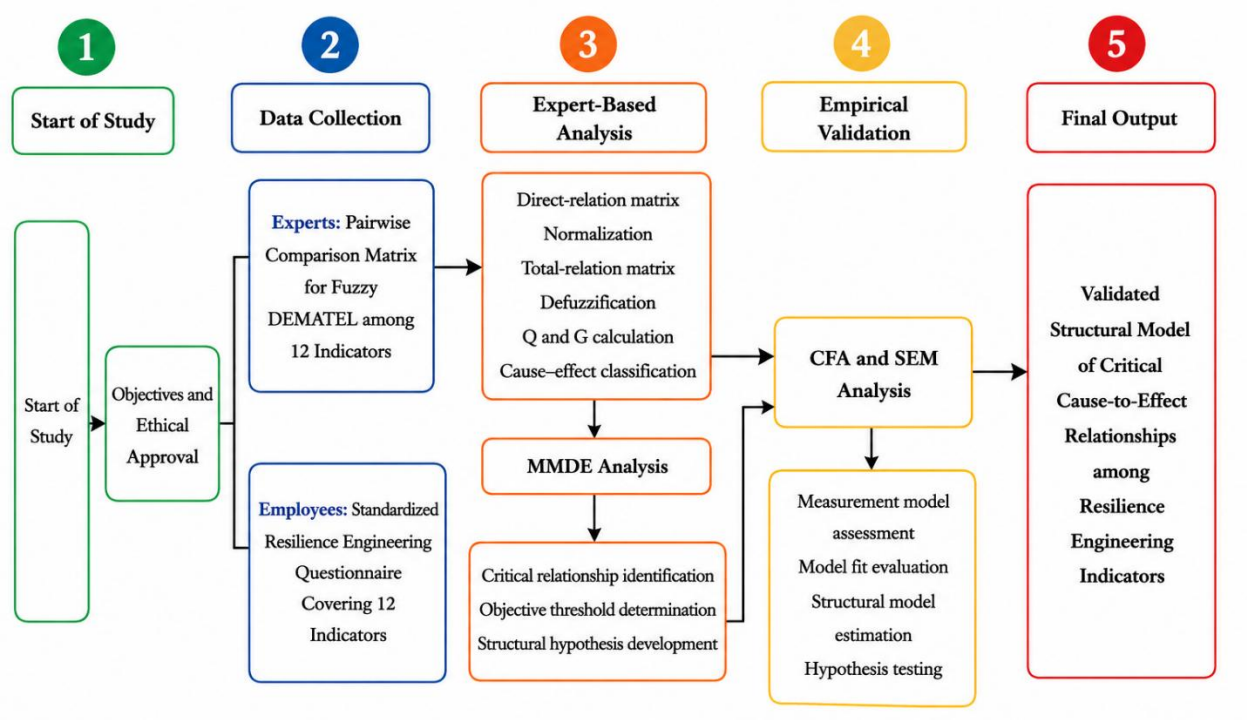


Figure 1. Overall analytical framework of the study, integrating expert-based fuzzy DEMATEL and MMDE analyses with employee-based CFA and SEM to identify and empirically validate critical relationships among resilience engineering indicators.

2.1. Ethical considerations

The objectives, procedures, and conditions of participation were clearly explained to all participants, including the employees participating in the questionnaire survey and the experts involved in the fuzzy DEMATEL phase. Written informed consent was obtained from all participants prior to data collection. Participation was entirely voluntary, and participants were informed that they could withdraw from the study at any time without penalty. All personal information and collected data were treated confidentially and used solely for research purposes. The study protocol was reviewed and approved by the Ethics Committee of Abadan University of Medical Sciences (Approval Code: IR.ABADANUMS.REC.1403.096). All methods were performed in accordance with the relevant guidelines and regulations.

2.2. Population and sampling

The employee population consisted of 1,124 individuals working in the selected petrochemical complex. Based on Cochran's formula with a 95% confidence level, the required sample size was estimated as 285 participants. Participants were selected using simple random sampling.

For the DEMATEL phase, 10 experts were recruited through purposive sampling supplemented by snowball sampling to ensure the inclusion of individuals with relevant professional and academic expertise. Inclusion criteria were: (1) a postgraduate qualification in health, safety, and environment (HSE) or a related field, (2) at least three years of industrial experience in safety consultancy or management, and (3) research or publication experience in resilience or safety. The experts' mean age was 48.4 years, with an average of 8.5 years of industrial experience. Written informed consent was obtained from all experts prior to their participation in the study.

2.3. Data collection instruments

Employee data were collected using the standardized questionnaire developed by Shirali et al. (2023), which consists of 121 items covering 12 resilience engineering indicators: buffering capacity (BC), management commitment (MC), reporting culture (RC), awareness (AW), preparedness (PR), flexibility (FL), self-organization (SO), teamwork (TW), redundancy (RD), learning culture (LC), fault-tolerance (FT), and anticipation (AN). The original validation study established the content and construct validity of the instrument and reported an overall Cronbach's alpha of 0.92[27].

A separate pairwise-comparison questionnaire was used for the fuzzy DEMATEL analysis. Experts evaluated the directional influence of each of the twelve resilience engineering indicators on every other indicator, resulting in a 12-by-12 direct-relation matrix in which the diagonal elements were fixed at zero to represent the absence of self-influence. Thus, both data-collection instruments addressed the same twelve indicators: the employee questionnaire measured the indicators using survey items, whereas the expert questionnaire elicited judgments regarding the directional interdependencies among them.

2.4. Data analysis

2.4.1. Fuzzy DEMATEL

Expert judgments were expressed using a five-point linguistic scale ranging from very low to very high. To account for the ambiguity and uncertainty inherent in linguistic assessments, the evaluations were converted into triangular fuzzy numbers (TFNs), based on fuzzy set theory introduced by Zadeh (1965). Fuzzy sets allow partial membership and therefore provide an appropriate framework for representing expert judgments under conditions of uncertainty [23,28].

A TFN is denoted by $\tilde{A} = (l, m, u)$, where l, m, and u represent the lower, most likely, and upper bounds, respectively (Soltani, Ahmadi, and Rashnoudi 2024). Its membership function is expressed as follows:

$$\mu_{\tilde{A}}(x) = \begin{cases} 0 & x < l \\ \dfrac{x - l}{m - l} & l \le x \le m \\ \dfrac{u - x}{u - m} & m \le x \le u \\ 0 & x > u \end{cases} \quad \text{(Eq. 1)}$$

The arithmetic properties of TFNs allow expert judgments to be aggregated and uncertainty to be propagated throughout the analytical procedure. For two TFNs, $\tilde{A}_1 = (l_1, m_1, u_1)$ and $\tilde{A}_2 = (l_2, m_2, u_2)$, the principal operations used in this study were as follows.

The addition operation:

$$\tilde{A}_1 + \tilde{A}_2 = (l_1 + l_2, m_1 + m_2, u_1 + u_2) \quad \text{(Eq. 2)}$$

The subtraction operation:

$$\tilde{A}_1 - \tilde{A}_2 = (l_1 - u_2, m_1 - m_2, u_1 - l_2) \quad \text{(Eq. 3)}$$

For the non-negative TFNs used in this study, the multiplication operation was expressed as:

$$\tilde{A}_1 \otimes \tilde{A}_2 = (l_1 l_2, m_1 m_2, u_1 u_2) \quad \text{(Eq. 4)}$$

The arithmetic operations of TFNs were used to aggregate expert judgments and to perform the subsequent fuzzy matrix calculations throughout the DEMATEL procedure. The five-point linguistic scale and its corresponding TFNs are presented in Table 1.

Table 1. Linguistic scale and corresponding TFNs

Linguistic term	TFN (l, m, u)
Very Low	(0, 0, 0.25)
Low	(0, 0.25, 0.5)
Medium	(0.25, 0.5, 0.75)
High	(0.5, 0.75, 1)
Very High	(0.75, 1, 1)

The zero TFN, $\tilde{0} = (0,0,0)$, was assigned to the diagonal elements of the direct-relation matrix to represent the absence of self-influence.

Fuzzy DEMATEL was employed to identify and quantify the interdependencies among the twelve resilience engineering indicators while accounting for the uncertainty inherent in expert judgments. The analytical procedure was conducted in six sequential steps, as described below.

Step 1. Formation of the initial direct-relation fuzzy matrix

The individual expert judgments were aggregated element-wise using the arithmetic mean. For each ordered pair of indicators i and j:

$$\tilde{e}_{ij} = \left(\frac{1}{p}\sum_{k=1}^{p} {l_{ij}}^{(k)}, \frac{1}{p}\sum_{k=1}^{p} {m_{ij}}^{(k)}, \frac{1}{p}\sum_{k=1}^{p} {u_{ij}}^{(k)} \right) \quad \text{(Eq. 5)}$$

The aggregated initial direct-relation fuzzy matrix was then expressed as:

$$\tilde{E} = \begin{bmatrix} \tilde{0} & \tilde{e}_{12} & \cdots & \tilde{e}_{1n} \\ \tilde{e}_{21} & \tilde{0} & \cdots & \tilde{e}_{2n} \\ \vdots & \vdots & \ddots & \vdots \\ \tilde{e}_{n1} & \tilde{e}_{n2} & \cdots & \tilde{0} \end{bmatrix} \quad \text{(Eq. 6)}$$

where $\tilde{E}$ denotes the aggregated initial direct-relation fuzzy matrix; each element $\tilde{e}_{ij} = (l_{ij}, m_{ij}, u_{ij})$ represents the aggregated fuzzy influence of indicator i on indicator j; ${\tilde{e}_{ij}}^{(k)}$ represents the judgment of expert k; p is the number of experts; and the diagonal elements are $\tilde{0} = (0,0,0)$. In the present analysis, n = 12, corresponding to the twelve resilience engineering indicators.

Step 2. Normalization of the direct-relation fuzzy matrix

The normalized direct-relation fuzzy matrix was calculated as:

$$\tilde{F} = \frac{\tilde{E}}{\gamma} \quad \text{(Eq. 7)}$$

The normalization coefficient was determined from the maximum row sum of the upper-bound values of the aggregated initial direct-relation fuzzy matrix:

$$\gamma = \max_{1 \le i \le n} \left(\sum_{j=1}^{n} u_{ij} \right) \quad \text{(Eq. 8)}$$

Accordingly:

$$\tilde{F} = \begin{bmatrix} \tilde{f}_{11} & \cdots & \tilde{f}_{1n} \\ \vdots & \ddots & \vdots \\ \tilde{f}_{n1} & \cdots & \tilde{f}_{nn} \end{bmatrix} \quad \text{(Eq. 9)}$$
$$\tilde{f}_{ij} = \frac{\tilde{e}_{ij}}{\gamma} = \left(\frac{l_{ij}}{\gamma}, \frac{m_{ij}}{\gamma}, \frac{u_{ij}}{\gamma} \right)$$

where F-tilde denotes the normalized direct-relation fuzzy matrix and γ is the normalization coefficient.

Step 3. Computation of the total-relation fuzzy matrix

The total-relation fuzzy matrix was represented as:

$$\tilde{T} = \begin{bmatrix} \tilde{t}_{11} & \cdots & \tilde{t}_{1n} \\ \vdots & \ddots & \vdots \\ \tilde{t}_{n1} & \cdots & \tilde{t}_{nn} \end{bmatrix} \quad \text{(Eq. 10)}$$
$$\tilde{t}_{ij} = \left(l'_{ij}, m'_{ij}, u'_{ij}\right)$$

Let F_l, F_m, and F_u denote the crisp matrices containing the lower, middle, and upper components of F-tilde, respectively. Their corresponding total-relation matrices were calculated as follows:

$$T_l = F_l(I - F_l)^{-1} \quad \text{(Eq. 11)}$$
$$T_m = F_m(I - F_m)^{-1} \quad \text{(Eq. 12)}$$
$$T_u = F_u(I - F_u)^{-1} \quad \text{(Eq. 13)}$$

where I denotes the identity matrix. The elements of T_l, T_m, and T_u correspond to l-prime subscript ij, m-prime subscript ij, and u-prime subscript ij, respectively.

Step 4. Defuzzification

The total-relation fuzzy matrix was converted into a crisp total-relation matrix using the following weighted defuzzification formula (Liu, Hu, and Huang 2024; Nyimbili, Erden, and Mwanaumo 2023):

$$t_{ij} = \frac{l'_{ij} + 2m'_{ij} + u'_{ij}}{4} \quad \text{(Eq. 14)}$$

The resulting crisp total-relation matrix was expressed as:

$$T = \begin{bmatrix} t_{11} & \cdots & t_{1n} \\ \vdots & \ddots & \vdots \\ t_{n1} & \cdots & t_{nn} \end{bmatrix} \quad \text{(Eq. 15)}$$

where t_{ij} represents the crisp total influence of indicator i on indicator j.

Step 5. Calculation of influence and dependence

For each indicator, the total influence exerted and the total influence received were calculated as follows for i = 1, 2, ..., n:

$$Q_i = \sum_{j=1}^{n} t_{ij} \quad \text{(Eq. 16)}$$

$$G_i = \sum_{j=1}^{n} t_{ji} \quad \text{(Eq. 17)}$$

where Q_i represents the total influence exerted by indicator i and corresponds to the sum of row i in the total-relation matrix, whereas G_i represents the total influence received by the same indicator and corresponds to the sum of column i.

Step 6. Determination of cause-and-effect roles

The prominence and relation indices were calculated as:

$$\text{Prominence}_i = Q_i + G_i \quad \text{(Eq. 18)}$$

$$\text{Relation}_i = Q_i - G_i \quad \text{(Eq. 19)}$$

The prominence index, $Q_i + G_i$, represents the overall involvement of an indicator within the system. The relation index, $Q_i - G_i$, indicates its net influence role. Indicators with positive $Q_i - G_i$ values were classified in the cause group, whereas those with negative values were classified in the effect group.

2.4.2. MMDE-based identification of critical relationships and hypothesis development

Following the fuzzy DEMATEL analysis, MMDE was employed to identify the most informative interrelationships among the twelve resilience engineering indicators and to establish an objective basis for structural hypothesis development. Because the DEMATEL total-relation matrix contains interdependencies of varying strength, directly incorporating all relationships into the subsequent structural model could result in an unnecessarily dense and less parsimonious specification. MMDE was therefore applied as an entropy-based procedure to determine an objective threshold and retain the most informative structure of the influence network, thereby reducing reliance on a subjectively selected cut-off value [26]. The unrounded defuzzified total-relation matrix was used as the input to the MMDE procedure, whereas rounded values were reported in the Results tables solely for presentation.

The MMDE procedure was implemented in the following sequential steps.

Step 1. Construction of the ordered influence set

The elements of the n × n defuzzified total-relation matrix were transformed into ordered triplets representing the magnitude of influence, the dispatch node, and the receive node:

$$T^{ord} = \{(t_{(s)}, x_{i_s}, x_{j_s}) : s = 1, \ldots, n^2\} \quad \text{(Eq. 20)}$$

where $t_{(s)}$denotes the s-th ordered total-influence value, x_{i_s}represents the corresponding dispatch node, and x_{j_s}represents the corresponding receive node. The triplets were arranged in descending order according to their total-influence values:

$$t_{(1)} \geq t_{(2)} \geq \ldots \geq t_{(n^2)} \quad \text{(Eq. 21)}$$

In the present study, **n = 12**, corresponding to the twelve resilience engineering indicators and yielding 144 ordered triplets in the complete total-relation matrix. Consistent with the MMDE procedure, all n^2elements of the total-relation matrix, including the diagonal elements, were included in the ordered sequence; self-relations were excluded only during the subsequent structural-hypothesis screening.

Step 2. Construction of the dispatch- and receive-node sequences

The ordered dispatch- and receive-node sequences were obtained from the second and third components of the ordered triplets, respectively:

$$T_D = (x_{i_1}, x_{i_2}, \ldots, x_{i_{n^2}}) \quad \text{(Eq. 22)}$$

$$T_R = (x_{j_1}, x_{j_2}, \ldots, x_{j_{n^2}}) \quad \text{(Eq. 23)}$$

For each t = 1, ..., n², the first t elements of the two ordered sequences were defined as:

$$T_D^{(t)} = (x_{i_1}, \ldots, x_{i_t}), \quad T_R^{(t)} = (x_{j_1}, \ldots, x_{j_t}) \quad \text{(Eq. 24)}$$

Step 3. Calculation of entropy and de-entropy

For each indicator x_r, its frequencies in the first t elements of the dispatch- and receive-node sequences were calculated as:

$$k_r^D(t) = \sum_{s=1}^{t} \mathrm{I}(i_s = \mathrm{r}), \quad k_r^R(t) = \sum_{s=1}^{t} \mathrm{I}(j_s = \mathrm{r}) \quad \text{(Eq. 25)}$$

where lndenotes the natural logarithm and 0ln 0was defined as zero. The corresponding probabilities were:

$$p_r^D(t) = \frac{k_r^D(t)}{t}, \quad p_r^R(t) = \frac{k_r^R(t)}{t} \qquad \text{(Eq. 26)}$$

The dispatch- and receive-node entropies were calculated as:

$$H_D(t) = -\sum_{r=1}^{n} p_r^D(t)\, ln\, p_r^D(t), \quad H_R(t) = -\sum_{r=1}^{n} p_r^R(t)\, ln\, p_r^R(t) \qquad \text{(Eq. 27)}$$

where 0 ln 0 was defined as zero. Let N_D(t) and N_R(t) denote the numbers of distinct dispatch and receive nodes appearing in the first t ordered triplets:

$$N_D(t) = \sum_{r=1}^{n} I(k_r^D(t) > 0), \quad N_R(t) = \sum_{r=1}^{n} I(k_r^R(t) > 0) \qquad \text{(Eq. 28)}$$

For each ordered subset, the maximum possible entropy was determined by the number of distinct nodes represented in that subset, rather than by the total number of study indicators:

$$H_D^{max}(t) = ln\, N_D(t), \quad H_R^{max}(t) = ln\, N_R(t) \qquad \text{(Eq. 29)}$$

The dispatch- and receive-node de-entropies were then calculated as:

$$H_D^{de}(t) = H_D^{max}(t) - H_D(t), \quad H_R^{de}(t) = H_R^{max}(t) - H_R(t) \qquad \text{(Eq. 30)}$$

Step 4. Calculation of mean de-entropy and identification of critical nodes

The corresponding mean de-entropy values were calculated by dividing de-entropy by the number of distinct nodes represented in the respective ordered prefix:

$$MDE_D(t) = \frac{H_D^{de}(t)}{N_D(t)}, \quad MDE_R(t) = \frac{H_R^{de}(t)}{N_R(t)} \tag{Eq. 31}$$

The positions yielding the maximum dispatch- and receive-node mean de-entropy values were identified as:

$$t_D^{max} = \arg\max_{1 \le t \le n^2} MDE_D(t), \quad t_R^{max} = \arg\max_{1 \le t \le n^2} MDE_R(t) \tag{Eq. 32}$$

The corresponding critical dispatch- and receive-node sets were defined as the sets of distinct nodes represented in the respective maximum-mean-de-entropy prefixes:

$$D^{\max} = \{x_{\mathrm{r}} : k_{\mathrm{r}}^{\mathrm{D}}(t^{\mathrm{Dmax}}) > 0\}, \quad R^{\max} = \{x_{\mathrm{r}} : k_{\mathrm{r}}^{\mathrm{R}}(t^{\mathrm{Rmax}}) > 0\} \tag{Eq. 33}$$

Step 5. Determination of the MMDE threshold

Let $D(u)$and $R(u)$denote the sets of distinct dispatch and receive nodes represented in the first $u$triplets of the ordered influence sequence, respectively:

$$D(u) = \{x_{\mathrm{is}} : 1 \le s \le u\}, \quad R(u) = \{x_{\mathrm{js}} : 1 \le s \le u\}$$

The threshold rank, denoted by u_{Th}, was defined as the smallest position in the ordered influence sequence at which all critical dispatch nodes in $D^{\max}$and all critical receive nodes in $R^{\max}$were simultaneously represented:

$$u_{Th} = min\{u : D^{max} \subseteq D(u), R^{max} \subseteq R(u)\} \quad \text{(Eq. 34)}$$

In other words, u_{Th}identifies the shortest prefix of the ordered triplet sequence that contains the complete sets of critical dispatch and receive nodes determined through the maximum mean de-entropy procedure.

$$\lambda = t_{(u_{Th})} = \min_{1 \le s \le u_{Th}} t_{(s)} \quad \text{(Eq. 35)}$$

The MMDE threshold, denoted by λ, was defined as the total-influence value at the threshold rank u_{Th}. Because the triplets were arranged in descending order, this value was equivalent to the minimum total-influence value among the first u_{Th}ordered triplets.

Relationships with total-influence values below the MMDE threshold were treated as relatively weak interdependencies, whereas those meeting or exceeding the threshold were retained for subsequent structural hypothesis development. The set of retained non-self relationships was defined as:

$$R_\lambda = \{(i,j) : i \neq j, t_{ij} \geq \lambda\} \quad \text{(Eq. 36)}$$

where $\mathcal{R}_\lambda$denotes the set of directed interrelationships satisfying the MMDE threshold, t_{ij}represents the total influence of indicator $i$on indicator j, and the condition $i \neq j$excludes self-relations from subsequent structural hypothesis development. The numerical value of the MMDE threshold obtained from the unrounded 12-indicator defuzzified total-relation matrix is reported in Section 3.3.

Step 6. Structural hypothesis development

The relationships retained through MMDE thresholding of the unrounded defuzzified total-relation matrix were used to formulate the a priori structural hypotheses for SEM analysis. Relationships with total-influence values equal to or greater than the MMDE threshold were considered eligible for structural model specification. The DEMATEL net-cause/net-effect classification was used to describe the relative roles of the indicators within the retained network and was not applied as an additional exclusion criterion. Therefore, both cross-group and within-group relationships satisfying the MMDE threshold were considered for subsequent empirical evaluation. The retained relationships were specified before SEM estimation, and no additional structural paths were introduced based on post hoc modification indices or empirical modification procedures.

2.4.3. Structural equation modeling (SEM)

Following the DEMATEL–MMDE analysis, the directional relationships retained through the MMDE thresholding procedure were translated into a priori research hypotheses and specified as structural paths. Accordingly, the structural model was developed based on the expert-derived causal network identified in the first phase of the study rather than through data-driven model specification. These predefined relationships were subsequently examined using covariance-based structural equation modeling (CB-SEM). Prior to model estimation, the employee survey data were screened for missing values, univariate and multivariate outliers, normality, and multicollinearity. Univariate outliers were identified using standardized scores, whereas multivariate outliers were assessed using Mahalanobis distance. Univariate normality was evaluated based on skewness and kurtosis, while multivariate normality was assessed using Mardia's coefficient. Multicollinearity was examined using the inter-indicator correlation matrix and variance inflation factors. Preliminary data screening and descriptive analyses were performed using IBM SPSS Statistics version 25.

The measurement and structural models were estimated using IBM SPSS Amos version 24 with the maximum likelihood estimation method. Confirmatory factor analysis (CFA) was conducted to evaluate the adequacy of the measurement model based on the magnitude and statistical significance of the standardized factor loadings. Subsequently, the hypothesized structural model, developed from the integrated DEMATEL–MMDE analysis, was estimated to examine the

proposed relationships. Model adequacy was evaluated using the chi-square statistic and its degrees of freedom, the chi-square-to-degrees-of-freedom ratio ($\chi^2/df < 3$), the comparative fit index (CFI ≥ 0.90), Tucker–Lewis index (TLI ≥ 0.90), incremental fit index (IFI ≥ 0.90), and the root mean square error of approximation (RMSEA < 0.08) with its 90% confidence interval. The proposed hypotheses were evaluated using standardized path coefficients, and p-values, with statistical significance established at $p < 0.05$. Squared multiple correlations were used to determine the variance explained in the endogenous constructs. Because multivariate non-normality was observed, bootstrap analyses were conducted using 5,000 resamples. The Bollen–Stine bootstrap was used to assess the robustness of overall model fit. In a separate bootstrap analysis without the Bollen–Stine option, bias-corrected 95% confidence intervals were calculated for the standardized direct, indirect, and total effects. An effect was considered statistically significant when its bootstrap confidence interval did not include zero.

3. Results

Following the presentation of participant characteristics and preliminary data assessment, the analytical results are reported in three sequential stages. First, the fuzzy DEMATEL findings are presented to characterize the direct and indirect influence structure among the twelve resilience engineering dimensions and to classify them into net-cause and net-effect groups. Second, the MMDE results are reported to identify the critical interrelationships retained for structural hypothesis development. Finally, the measurement and structural models are evaluated using CFA and SEM to empirically test the predefined relationships derived from the integrated DEMATEL–MMDE procedure.

3.1. Participant Characteristics and Preliminary Data Assessment

A total of 343 employees participated in the study, of whom 77.8% were men. Among participants, 47.8% were aged 25–35 years and 38.1% were aged 36–46 years. Nearly half of the participants held a bachelor's degree (48.7%), and most were employed on a contractual basis (61.5%). Regarding work experience, the largest proportion had more than 16 years of experience (31.0%). No missing values were identified in the dataset. Skewness and kurtosis values indicated acceptable univariate normality; however, multivariate normality was not achieved, as indicated

by Mardia's multivariate kurtosis critical ratio (CR = 10.098). No influential univariate or multivariate outliers were identified based on standardized scores and Mahalanobis distance. Multicollinearity was not observed based on inter-construct correlations and variance inflation factors.

3.2. Fuzzy DEMATEL results

The interrelationships among the twelve resilience engineering indicators were examined using fuzzy DEMATEL based on the judgments of ten experts. The expert assessments were aggregated to obtain the initial direct-relation fuzzy matrix, representing the perceived directional influence of each indicator on the others. The resulting matrix is presented in Table 2. The initial direct-relation fuzzy matrix was subsequently normalized using a normalization coefficient of $\gamma = 10.225$ to ensure comparability of the influence values across the indicator system. The resulting normalized direct-relation fuzzy matrix is presented in Table 3. The normalized matrix was then used to calculate the total-relation fuzzy matrix, which captures both the direct and indirect influences among the indicators. The resulting total-relation fuzzy matrix is presented in Table 4. Following defuzzification, the crisp total-relation matrix was obtained, as presented in Table 5. Each element t_{ij}represents the cumulative direct and indirect influence exerted by indicator $i$on indicator j. The strongest off-diagonal total influence was observed from AW to FT $(t_{ij} = 0.3086)$, followed by AW to AN (0.3010), AW to PR (0.2976), BC to PR (0.2956), and AW to FL (0.2940). Four of the five strongest off-diagonal relationships originated from AW, whereas the relationship from BC to PR had the fourth-highest value. The total influence exerted by each indicator (Q_i)_, the total influence received (G_i), the prominence index ($Q_i + G_i$), and the relation index ($Q_i - G_i$) are presented jointly in Figure 2. As shown in Figure 2a, AW exhibited the highest total influence ($Q_i = 3.1816$), followed by BC (2.8955) and PR (2.8618).

Table 2. Aggregated initial direct-relation fuzzy matrix of the twelve resilience engineering indicators based on expert judgments												
Indicator	**BC**	**MC**	**RC**	**AW**	**PR**	**FL**	**SO**	**TW**	**RD**	**LC**	**FT**	**AN**
BC	(0,0,0)	(0,0.23,0.47)	(0.03,0.25,0.50)	(0.62,0.88,0.95)	(0.72,0.97,1)	(0.53,0.78,1)	(0.47,0.72,0.97)	(0.65,0.88,0.93)	(0.07,0.33,0.55)	(0.65,0.90,0.97)	(0.53,0.78,1)	(0.38,0.62,0.88)
MC	(0.15,0.35,0.57)	(0,0,0)	(0.28,0.53,0.78)	(0.28,0.53,0.78)	(0.30,0.55,0.80)	(0.47,0.72,0.97)	(0.75,1,1)	(0.35,0.60,0.82)	(0.42,0.68,0.93)	(0.10,0.30,0.55)	(0.25,0.50,0.75)	(0.40,0.62,0.80)
RC	(0.28,0.53,0.78)	(0.05,0.30,0.55)	(0,0,0)	(0.30,0.55,0.80)	(0.53,0.78,1)	(0.30,0.55,0.78)	(0.30,0.55,0.80)	(0.30,0.55,0.78)	(0.47,0.72,0.95)	(0.50,0.75,1)	(0.03,0.28,0.53)	(0.60,0.85,1)
AW	(0.60,0.85,0.97)	(0.23,0.45,0.70)	(0.50,0.75,1)	(0,0,0)	(0.47,0.70,0.93)	(0.50,0.75,0.97)	(0.45,0.70,0.95)	(0.42,0.68,0.93)	(0.45,0.70,0.93)	(0.42,0.68,0.88)	(0.70,0.95,0.97)	(0.70,0.95,1)
PR	(0.53,0.78,0.97)	(0.28,0.53,0.78)	(0.17,0.42,0.62)	(0.20,0.45,0.70)	(0,0,0)	(0.47,0.72,0.95)	(0.55,0.80,1)	(0.25,0.50,0.72)	(0.60,0.85,1)	(0.25,0.50,0.75)	(0.50,0.75,0.97)	(0.50,0.75,1)
FL	(0.72,0.97,1)	(0.05,0.30,0.55)	(0.05,0.30,0.55)	(0.38,0.62,0.82)	(0.55,0.80,1)	(0,0,0)	(0.33,0.57,0.80)	(0.30,0.55,0.80)	(0.50,0.75,1)	(0.15,0.40,0.60)	(0.72,0.97,1)	(0.33,0.57,0.78)
SO	(0.28,0.53,0.78)	(0.23,0.47,0.72)	(0.28,0.53,0.78)	(0.28,0.53,0.78)	(0.25,0.47,0.70)	(0.23,0.45,0.70)	(0,0,0)	(0.50,0.75,1)	(0.30,0.55,0.78)	(0.28,0.53,0.78)	(0.33,0.57,0.80)	(0.47,0.72,0.90)
TW	(0.25,0.50,0.75)	(0.35,0.60,0.80)	(0.47,0.72,0.97)	(0.23,0.47,0.72)	(0.50,0.75,0.95)	(0.45,0.68,0.93)	(0.30,0.55,0.78)	(0,0,0)	(0.25,0.50,0.75)	(0.20,0.45,0.70)	(0.28,0.53,0.75)	(0.42,0.68,0.88)
RD	(0.70,0.95,1)	(0.03,0.28,0.53)	(0.03,0.28,0.53)	(0.07,0.30,0.53)	(0.53,0.78,1)	(0.75,1,1)	(0.28,0.50,0.72)	(0.07,0.28,0.50)	(0,0,0)	(0.20,0.40,0.62)	(0.53,0.78,1)	(0.30,0.55,0.78)
LC	(0.25,0.50,0.75)	(0.25,0.50,0.75)	(0.53,0.78,1)	(0.55,0.80,1)	(0.50,0.75,1)	(0.23,0.47,0.72)	(0.35,0.60,0.82)	(0.25,0.50,0.75)	(0.23,0.47,0.72)	(0,0,0)	(0.38,0.62,0.88)	(0.28,0.50,0.70)
FT	(0.42,0.65,0.85)	(0.05,0.30,0.55)	(0.10,0.35,0.57)	(0.10,0.33,0.55)	(0.23,0.47,0.72)	(0.50,0.75,1)	(0.17,0.42,0.68)	(0,0.25,0.50)	(0.55,0.80,1)	(0.05,0.30,0.55)	(0,0,0)	(0.28,0.50,0.70)
AN	(0.25,0.50,0.75)	(0.12,0.38,0.60)	(0,0.23,0.47)	(0.47,0.72,0.97)	(0.45,0.70,0.95)	(0.25,0.50,0.75)	(0.50,0.75,1)	(0.23,0.47,0.70)	(0.28,0.53,0.78)	(0.20,0.45,0.65)	(0.47,0.72,0.97)	(0,0,0)

Note: Values represent the element-wise arithmetic means of the ten experts' assessments and are expressed as triangular fuzzy numbers (TFNs) (l,m,u), rounded to two decimal places for presentation. Diagonal elements were fixed at (0,0,0) to represent the absence of self-influence. BC, Buffering Capacity; MC, Management Commitment; RC, Reporting Culture; AW, Awareness; PR, Preparedness; FL, Flexibility; SO, Self-organization; TW, Teamwork; RD, Redundancy; LC, Learning Culture; FT, Fault-tolerance; AN, Anticipation.

Table 3. Normalized direct-relation fuzzy matrix of the twelve resilience engineering indicators												
Indicator	**BC**	**MC**	**RC**	**AW**	**PR**	**FL**	**SO**	**TW**	**RD**	**LC**	**FT**	**AN**
BC	(0,0,0)	(0,0.022,0.046)	(0.002,0.024,0.049)	(0.061,0.086,0.093)	(0.071,0.095,0.098)	(0.051,0.076,0.098)	(0.046,0.071,0.095)	(0.064,0.086,0.090)	(0.007,0.032,0.054)	(0.064,0.088,0.095)	(0.051,0.076,0.098)	(0.037,0.061,0.086)
MC	(0.015,0.034,0.056)	(0,0,0)	(0.027,0.051,0.076)	(0.027,0.051,0.076)	(0.029,0.054,0.078)	(0.046,0.071,0.095)	(0.073,0.098,0.098)	(0.034,0.059,0.081)	(0.042,0.066,0.090)	(0.010,0.029,0.054)	(0.024,0.049,0.073)	(0.039,0.061,0.078)
RC	(0.027,0.051,0.076)	(0.005,0.029,0.054)	(0,0,0)	(0.029,0.054,0.078)	(0.051,0.076,0.098)	(0.029,0.054,0.076)	(0.029,0.054,0.078)	(0.029,0.054,0.076)	(0.046,0.071,0.093)	(0.049,0.073,0.098)	(0.002,0.027,0.051)	(0.059,0.083,0.098)
AW	(0.059,0.083,0.095)	(0.022,0.044,0.068)	(0.049,0.073,0.098)	(0,0,0)	(0.046,0.068,0.090)	(0.049,0.073,0.095)	(0.044,0.068,0.093)	(0.042,0.066,0.090)	(0.044,0.068,0.090)	(0.042,0.066,0.086)	(0.068,0.093,0.095)	(0.068,0.093,0.098)
PR	(0.051,0.076,0.095)	(0.027,0.051,0.076)	(0.017,0.042,0.061)	(0.020,0.044,0.068)	(0,0,0)	(0.046,0.071,0.093)	(0.054,0.078,0.098)	(0.024,0.049,0.071)	(0.059,0.083,0.098)	(0.024,0.049,0.073)	(0.049,0.073,0.095)	(0.049,0.073,0.098)
FL	(0.071,0.095,0.098)	(0.005,0.029,0.054)	(0.005,0.029,0.054)	(0.037,0.061,0.081)	(0.054,0.078,0.098)	(0,0,0)	(0.032,0.056,0.078)	(0.029,0.054,0.078)	(0.049,0.073,0.098)	(0.015,0.039,0.059)	(0.071,0.095,0.098)	(0.032,0.056,0.076)
SO	(0.027,0.051,0.076)	(0.022,0.046,0.071)	(0.027,0.051,0.076)	(0.027,0.051,0.076)	(0.024,0.046,0.068)	(0.022,0.044,0.068)	(0,0,0)	(0.049,0.073,0.098)	(0.029,0.054,0.076)	(0.027,0.051,0.076)	(0.032,0.056,0.078)	(0.046,0.071,0.088)
TW	(0.024,0.049,0.073)	(0.034,0.059,0.078)	(0.046,0.071,0.095)	(0.022,0.046,0.071)	(0.049,0.073,0.093)	(0.044,0.066,0.090)	(0.029,0.054,0.076)	(0,0,0)	(0.024,0.049,0.073)	(0.020,0.044,0.068)	(0.027,0.051,0.073)	(0.042,0.066,0.086)
RD	(0.068,0.093,0.098)	(0.002,0.027,0.051)	(0.002,0.027,0.051)	(0.007,0.029,0.051)	(0.051,0.076,0.098)	(0.073,0.098,0.098)	(0.027,0.049,0.071)	(0.007,0.027,0.049)	(0,0,0)	(0.020,0.039,0.061)	(0.051,0.076,0.098)	(0.029,0.054,0.076)
LC	(0.024,0.049,0.073)	(0.024,0.049,0.073)	(0.051,0.076,0.098)	(0.054,0.078,0.098)	(0.049,0.073,0.098)	(0.022,0.046,0.071)	(0.034,0.059,0.081)	(0.024,0.049,0.073)	(0.022,0.046,0.071)	(0,0,0)	(0.037,0.061,0.086)	(0.027,0.049,0.068)
FT	(0.042,0.064,0.083)	(0.005,0.029,0.054)	(0.010,0.034,0.056)	(0.010,0.032,0.054)	(0.022,0.046,0.071)	(0.049,0.073,0.098)	(0.017,0.042,0.066)	(0,0.024,0.049)	(0.054,0.078,0.098)	(0.005,0.029,0.054)	(0,0,0)	(0.027,0.049,0.068)
AN	(0.024,0.049,0.073)	(0.012,0.037,0.059)	(0,0.022,0.046)	(0.046,0.071,0.095)	(0.044,0.068,0.093)	(0.024,0.049,0.073)	(0.049,0.073,0.098)	(0.022,0.046,0.068)	(0.027,0.051,0.076)	(0.020,0.044,0.064)	(0.046,0.071,0.095)	(0,0,0)

Note: Values are expressed as normalized triangular fuzzy numbers (TFNs) (l,m,u) and rounded to three decimal places for presentation.

The normalization coefficient was $\gamma = 10.225$.

Table 4. Total-relation fuzzy matrix of the twelve resilience engineering indicators												
Indicator	**BC**	**MC**	**RC**	**AW**	**PR**	**FL**	**SO**	**TW**	**RD**	**LC**	**FT**	**AN**
BC	(0.03,0.12,0.53)	(0.01,0.10,0.45)	(0.02,0.11,0.49)	(0.08,0.18,0.57)	(0.10,0.21,0.65)	(0.08,0.19,0.64)	(0.07,0.18,0.63)	(0.08,0.18,0.56)	(0.03,0.15,0.58)	(0.08,0.18,0.55)	(0.08,0.20,0.64)	(0.06,0.18,0.61)
MC	(0.04,0.14,0.55)	(0.01,0.06,0.38)	(0.04,0.12,0.49)	(0.04,0.14,0.53)	(0.05,0.16,0.61)	(0.07,0.17,0.61)	(0.09,0.19,0.60)	(0.05,0.14,0.53)	(0.06,0.16,0.59)	(0.02,0.11,0.49)	(0.05,0.16,0.59)	(0.06,0.16,0.58)
RC	(0.05,0.15,0.58)	(0.01,0.09,0.44)	(0.01,0.07,0.43)	(0.05,0.14,0.55)	(0.07,0.18,0.64)	(0.05,0.16,0.61)	(0.05,0.15,0.60)	(0.04,0.14,0.54)	(0.06,0.17,0.60)	(0.06,0.15,0.54)	(0.03,0.14,0.58)	(0.08,0.18,0.61)
AW	(0.09,0.21,0.66)	(0.03,0.12,0.51)	(0.06,0.16,0.57)	(0.03,0.11,0.54)	(0.08,0.20,0.70)	(0.08,0.20,0.69)	(0.07,0.19,0.67)	(0.06,0.17,0.61)	(0.07,0.19,0.67)	(0.06,0.17,0.58)	(0.10,0.22,0.69)	(0.10,0.22,0.67)
PR	(0.08,0.19,0.62)	(0.03,0.12,0.48)	(0.03,0.12,0.50)	(0.04,0.14,0.56)	(0.03,0.12,0.58)	(0.07,0.18,0.65)	(0.08,0.18,0.64)	(0.04,0.14,0.55)	(0.08,0.19,0.63)	(0.04,0.14,0.54)	(0.08,0.19,0.65)	(0.07,0.18,0.63)
FL	(0.09,0.20,0.60)	(0.01,0.10,0.44)	(0.02,0.11,0.47)	(0.05,0.15,0.54)	(0.08,0.19,0.63)	(0.03,0.12,0.53)	(0.05,0.16,0.59)	(0.05,0.14,0.53)	(0.07,0.17,0.60)	(0.03,0.13,0.50)	(0.10,0.21,0.62)	(0.05,0.16,0.58)
SO	(0.05,0.15,0.57)	(0.03,0.11,0.45)	(0.04,0.12,0.49)	(0.04,0.13,0.53)	(0.05,0.15,0.60)	(0.04,0.14,0.59)	(0.02,0.10,0.51)	(0.06,0.15,0.54)	(0.05,0.15,0.57)	(0.04,0.13,0.50)	(0.05,0.16,0.59)	(0.07,0.17,0.58)
TW	(0.05,0.15,0.58)	(0.04,0.12,0.46)	(0.06,0.14,0.52)	(0.04,0.13,0.54)	(0.07,0.18,0.64)	(0.06,0.17,0.62)	(0.05,0.15,0.59)	(0.02,0.09,0.47)	(0.05,0.15,0.59)	(0.03,0.12,0.51)	(0.05,0.16,0.60)	(0.06,0.17,0.60)
RD	(0.09,0.19,0.56)	(0.01,0.09,0.41)	(0.01,0.09,0.44)	(0.02,0.12,0.48)	(0.07,0.18,0.59)	(0.09,0.19,0.58)	(0.05,0.14,0.55)	(0.02,0.11,0.47)	(0.02,0.10,0.47)	(0.03,0.12,0.47)	(0.07,0.18,0.58)	(0.05,0.15,0.54)
LC	(0.05,0.15,0.59)	(0.03,0.11,0.47)	(0.06,0.15,0.53)	(0.07,0.16,0.57)	(0.07,0.18,0.65)	(0.05,0.15,0.61)	(0.06,0.16,0.61)	(0.04,0.14,0.54)	(0.04,0.15,0.59)	(0.02,0.08,0.46)	(0.06,0.17,0.62)	(0.05,0.16,0.59)
FT	(0.06,0.15,0.52)	(0.01,0.08,0.39)	(0.01,0.09,0.42)	(0.02,0.10,0.46)	(0.04,0.14,0.54)	(0.06,0.16,0.55)	(0.03,0.12,0.51)	(0.01,0.09,0.45)	(0.07,0.15,0.53)	(0.02,0.10,0.44)	(0.02,0.09,0.46)	(0.04,0.13,0.51)
AN	(0.04,0.15,0.56)	(0.02,0.10,0.43)	(0.01,0.09,0.46)	(0.06,0.15,0.54)	(0.06,0.17,0.61)	(0.04,0.15,0.59)	(0.07,0.16,0.59)	(0.04,0.13,0.51)	(0.04,0.14,0.57)	(0.03,0.12,0.49)	(0.07,0.17,0.60)	(0.02,0.10,0.50)

Note: Values are expressed as triangular fuzzy numbers (TFNs) (l,m,u), representing the cumulative direct and indirect influences among the indicators, and are rounded to two decimal places for presentation. Calculations were performed using the unrounded matrix values.

Table 5. Defuzzified total-relation matrix of the twelve resilience engineering indicators												
Indicator	**BC**	**MC**	**RC**	**AW**	**PR**	**FL**	**SO**	**TW**	**RD**	**LC**	**FT**	**AN**
BC	0.1989	0.1636	0.1821	0.2549	0.2956	0.2756	0.2657	0.2507	0.2271	0.2446	0.2789	0.2577
MC	0.2160	0.1293	0.1917	0.2120	0.2452	0.2553	0.2686	0.2156	0.2426	0.1826	0.2366	0.2405
RC	0.2349	0.1610	0.1468	0.2197	0.2703	0.2434	0.2388	0.2145	0.2495	0.2260	0.2218	0.2630
AW	0.2920	0.1952	0.2381	0.1965	0.2976	0.2940	0.2828	0.2531	0.2786	0.2441	0.3086	0.3010
PR	0.2670	0.1874	0.1920	0.2198	0.2113	0.2713	0.2703	0.2196	0.2699	0.2120	0.2748	0.2665
FL	0.2731	0.1609	0.1750	0.2257	0.2737	0.1975	0.2418	0.2165	0.2547	0.1953	0.2819	0.2416
SO	0.2268	0.1718	0.1904	0.2105	0.2363	0.2289	0.1807	0.2265	0.2274	0.1996	0.2391	0.2453
TW	0.2320	0.1862	0.2125	0.2121	0.2666	0.2556	0.2384	0.1642	0.2314	0.1988	0.2419	0.2488
RD	0.2557	0.1470	0.1589	0.1847	0.2551	0.2649	0.2198	0.1790	0.1707	0.1833	0.2523	0.2229
LC	0.2353	0.1808	0.2202	0.2422	0.2707	0.2409	0.2456	0.2135	0.2324	0.1603	0.2544	0.2379
FT	0.2171	0.1386	0.1536	0.1720	0.2124	0.2321	0.1969	0.1619	0.2267	0.1605	0.1649	0.2027
AN	0.2237	0.1608	0.1622	0.2253	0.2525	0.2307	0.2467	0.1998	0.2242	0.1897	0.2520	0.1786

Note: Values are reported to four decimal places for presentation. The Q_i, G_i, $Q_i + G_i$, and $Q_i - G_i$ indices and the MMDE procedure were calculated using the unrounded defuzzified total-relation matrix.

Figure 2b presents the total influence received by each indicator. PR showed the highest total dependence on the remaining indicators (G_i=3.0874), followed by FT (3.0073) and FL (2.9903). The prominence index ($Q_i + G_i$), which reflects the overall involvement of an indicator by jointly considering the influence exerted and received, is shown in Figure 2c. PR had the highest prominence value ($Q_i + G_i$=5.9492), followed by BC (5.7679), AW (5.7569), and FL (5.7280), whereas MC had the lowest prominence value (4.6187). Thus, PR represented the indicator with the greatest overall involvement in the resilience engineering influence structure. The relation index ($Q_i - G_i$), shown in Figure 2d, was used to distinguish the net-cause and net-effect roles of the indicators. Positive values indicate indicators that exert greater total influence than they receive, whereas negative values indicate indicators that receive greater total influence than they exert. MC exhibited the highest positive relation value ($Q_i - G_i$=0.6533), followed by AW (0.6062) and RC (0.4664), identifying MC as the strongest net-cause indicator. BC remained in the net-cause group but exhibited only a small positive net influence (0.023). Conversely, FT showed the most negative relation value (-0.7679), identifying it as the strongest net-effect indicator, followed by AN (-0.3604) and RD (-0.3411). The final net-cause and net-effect classification derived from the $Q_i - G_i$ values is summarized in Table 6. BC, MC, RC, AW, TW, and LC were classified as net-cause indicators, indicating that their total influence exerted exceeded their total influence received. In contrast, PR, FL, SO, RD, FT, and AN were classified as net-effect indicators, indicating that they received greater total influence from the system than they exerted. Among the net-cause indicators, MC exhibited the highest relation value, followed by AW and RC. Conversely, FT showed the most negative relation value and was identified as the strongest net-effect indicator.

The resulting cause–effect diagram is presented in Figure 3. The horizontal axis represents prominence, expressed as $Q_i + G_i$, whereas the vertical axis represents relation, expressed as $Q_i - G_i$. Accordingly, each indicator was positioned according to its overall involvement in the influence structure and its net influence role. The vertical reference line represents the mean prominence value of 5.3814, while the horizontal zero line separates the net-cause indicators from the net-effect indicators. Indicators positioned above the zero line exerted greater total influence than they received, whereas those positioned below the line received greater total influence than they exerted.

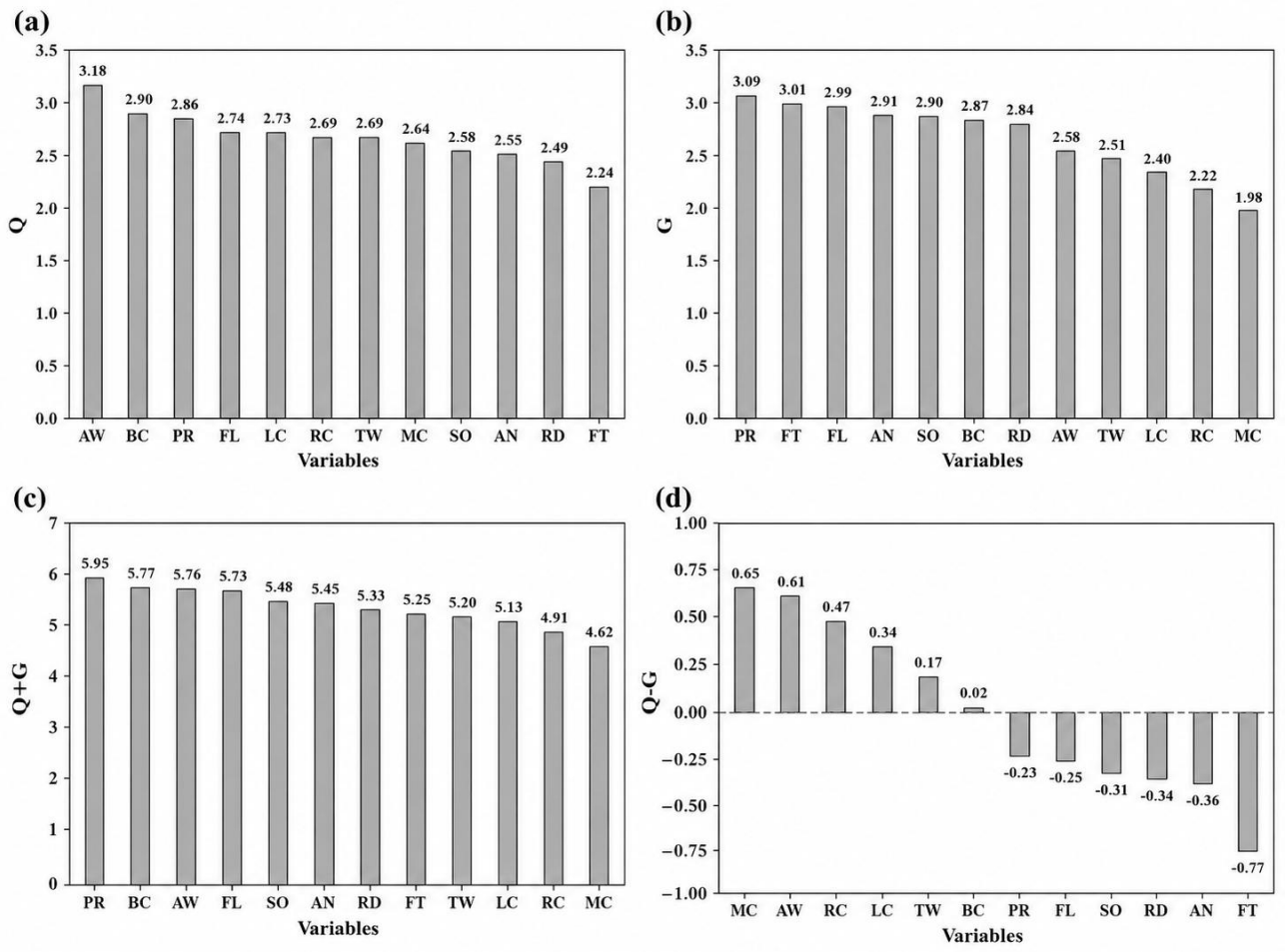


Figure 2. Results of the fuzzy DEMATEL analysis for the resilience engineering variables: (a) total influence exerted (Q_i), (b) total influence received (G_i), (c) prominence ($Q_i + G_i$), and (d) relation ($Q_i - G_i$). Positive values of $Q_i - G_i$ indicate variables belonging to the cause group, whereas negative values indicate variables belonging to the effect group.

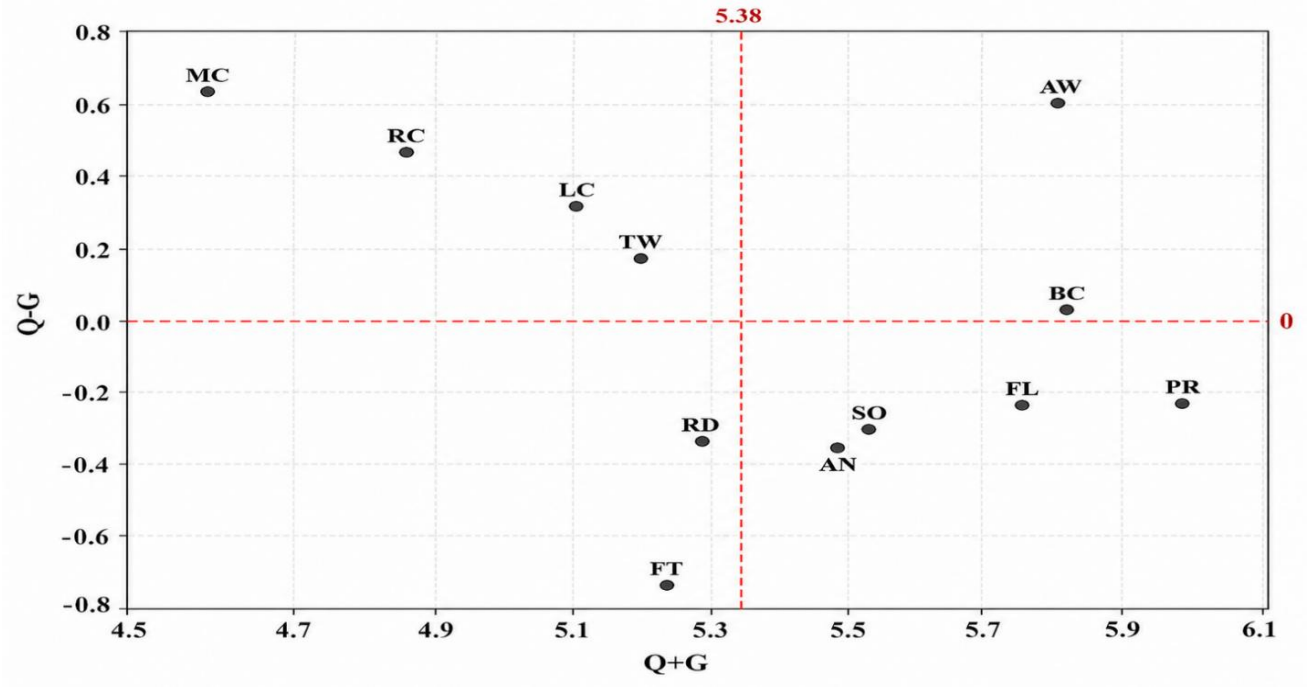


Figure 3. Cause–effect diagram of the resilience engineering variables based on fuzzy DEMATEL. The horizontal axis denotes prominence ($Q_i + G_i$) and the vertical axis relation ($Q_i - G_i$); positive and negative relation values identify cause and effect variables, respectively. The vertical dashed line represents the mean prominence value of 5.381.

Table 6. DEMATEL influence indices and net-cause/net-effect classification of the resilience engineering indicators

Indicator	Q_i	G_i	$Q_i + G_i$	$Q_i - G_i$	Role
Buffering Capacity (BC)	2.8955	2.8725	5.7679	0.0230	Net-cause
Management Commitment (MC)	2.6360	1.9827	4.6187	0.6533	Net-cause
Reporting Culture (RC)	2.6897	2.2233	4.9131	0.4664	Net-cause
Awareness (AW)	3.1816	2.5754	5.7569	0.6062	Net-cause
Preparedness (PR)	2.8618	3.0874	5.9492	−0.2257	Net-effect
Flexibility (FL)	2.7378	2.9903	5.7280	−0.2525	Net-effect
Self-organization (SO)	2.5832	2.8960	5.4792	−0.3128	Net-effect
Teamwork (TW)	2.6888	2.5149	5.2037	0.1739	Net-cause
Redundancy (RD)	2.4941	2.8352	5.3294	−0.3411	Net-effect
Learning Culture (LC)	2.7344	2.3968	5.1312	0.3376	Net-cause
Fault-tolerance (FT)	2.2393	3.0073	5.2466	−0.7679	Net-effect
Anticipation (AN)	2.5461	2.9064	5.4525	−0.3604	Net-effect

Overall, the fuzzy DEMATEL analysis quantified the expert-derived direct and indirect influence structure among the twelve resilience engineering indicators and classified them according to their net-cause and net-effect roles. MC, AW, and RC exhibited the highest positive relation values, identifying them as the strongest net-cause indicators, whereas FT, AN, and RD showed the most negative relation values and represented the strongest net-effect indicators. The unrounded defuzzified total-relation matrix was subsequently analyzed using MMDE to identify the critical interrelationships retained for structural hypothesis development.

3.3. MMDE-Based Relationship Selection

The MMDE procedure was applied to the 12 × 12 defuzzified total-relation matrix underlying Table 5. Separate mean de-entropy profiles were generated for the ordered dispatch- and receive-node sequences. The dispatch-node profile reached its maximum at rank 7, identifying AW and BC as the critical dispatch nodes, whereas the receive-node profile reached its maximum at rank 17, identifying FT, AN, PR, FL, BC, SO, and RD as the critical receive nodes (Figure 4).

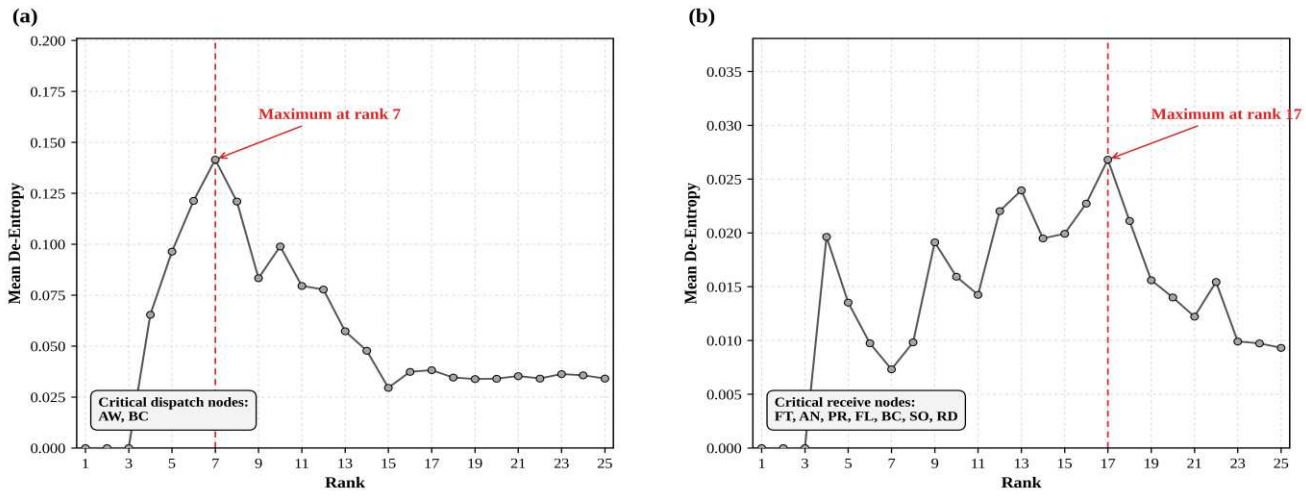


Figure 4. Mean de-entropy profiles used for MMDE relationship selection: (a) dispatch-node sequence and (b) receive-node sequence. The dashed red lines indicate the maximum mean de-entropy values at ranks 7 and 17, respectively.

Following MMDE processing of all matrix elements, the 12 diagonal self-relations were excluded from structural screening, leaving 132 candidate directed relationships. The shortest ordered prefix containing all critical dispatch and receive nodes ended at rank 10, corresponding to a total-influence

threshold of 0.2786. Relationships with total-influence values equal to or greater than this threshold were retained, reducing the candidate set to 10 critical interdependencies; the remaining 122 relationships were excluded (Figure 5).

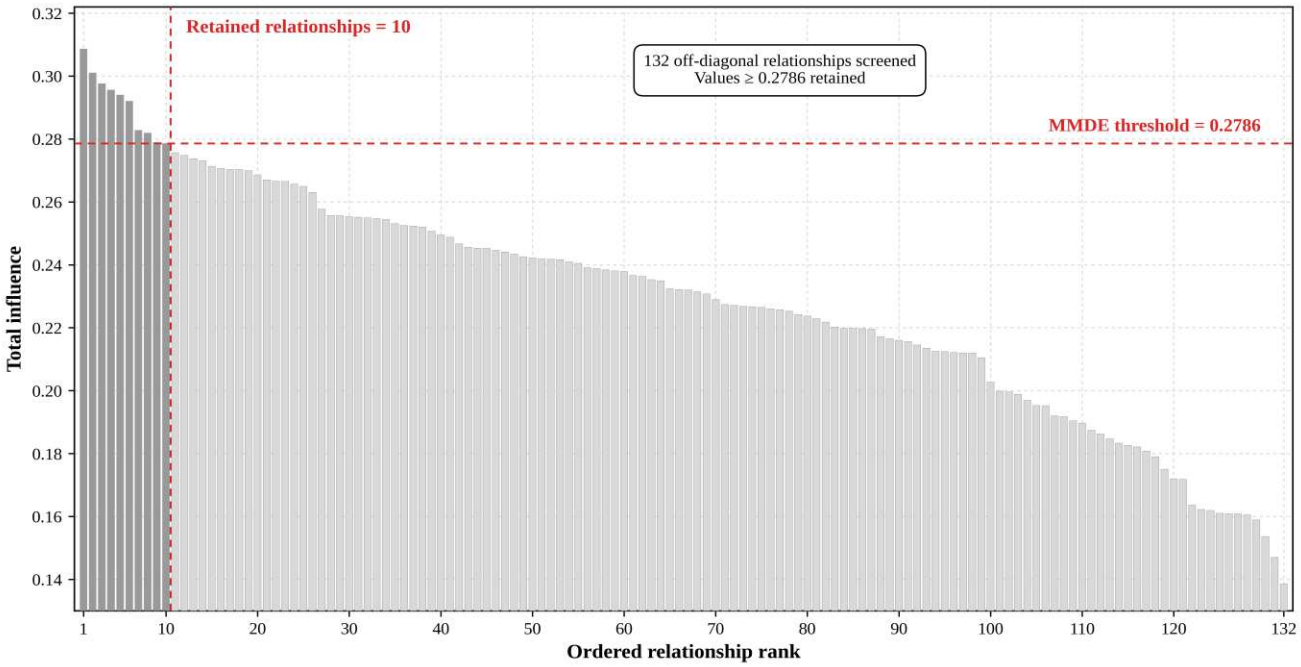


Figure 5. Ordered off-diagonal total-influence values and the MMDE threshold. The first 10 relationships met or exceeded the threshold of 0.2786, whereas the remaining 122 relationships were excluded.

Table 7. MMDE-retained structural relationships

Rank	Hypothesis	Structural relationship	Total influence	Relationship type
1	H7	AW to FT	0.3086	Net-cause to net-effect
2	H8	AW to AN	0.3010	Net-cause to net-effect
3	H3	AW to PR	0.2976	Net-cause to net-effect
4	H1	BC to PR	0.2956	Net-cause to net-effect
5	H4	AW to FL	0.2940	Net-cause to net-effect
6	H9	AW to BC	0.2920	Within net-cause
7	H5	AW to SO	0.2828	Net-cause to net-effect
8	H10	FL to FT	0.2819	Within net-effect
9	H2	BC to FT	0.2789	Net-cause to net-effect
10	H6	AW to RD	0.2786	Net-cause to net-effect

The DEMATEL net-cause/net-effect classification was used only to describe the positions of the dimensions within the retained structure and was not applied as an additional selection criterion. Eight retained relationships linked a net-cause dimension to a net-effect dimension; AW to BC represented a within-net-cause relationship, and FL to FT represented a within-net-effect relationship. AW was the source node in seven retained relationships, BC in two, and FL in one. These 10 relationships constituted the prespecified structural model subsequently evaluated using SEM (Figure 6), and no additional paths were introduced on the basis of post hoc modification indices.

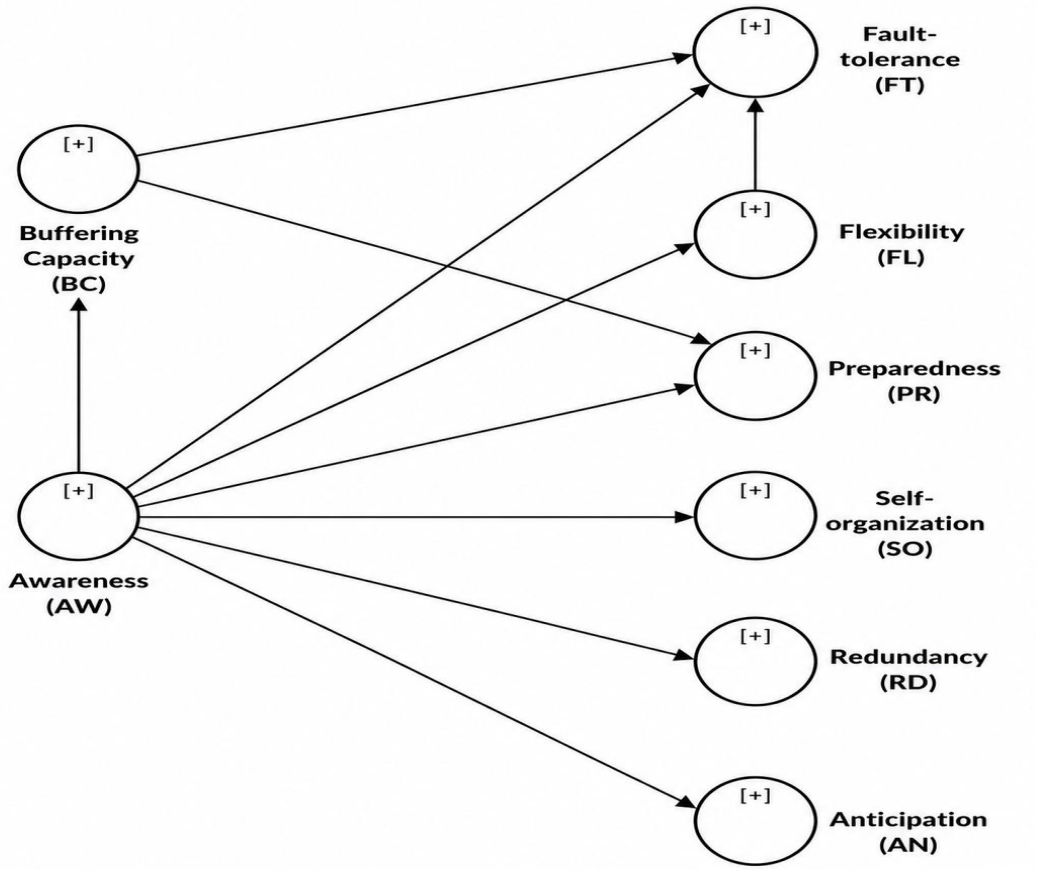


Figure 6. Structural model derived from the 10 MMDE-retained relationships.

3.4. Structural Equation Modeling

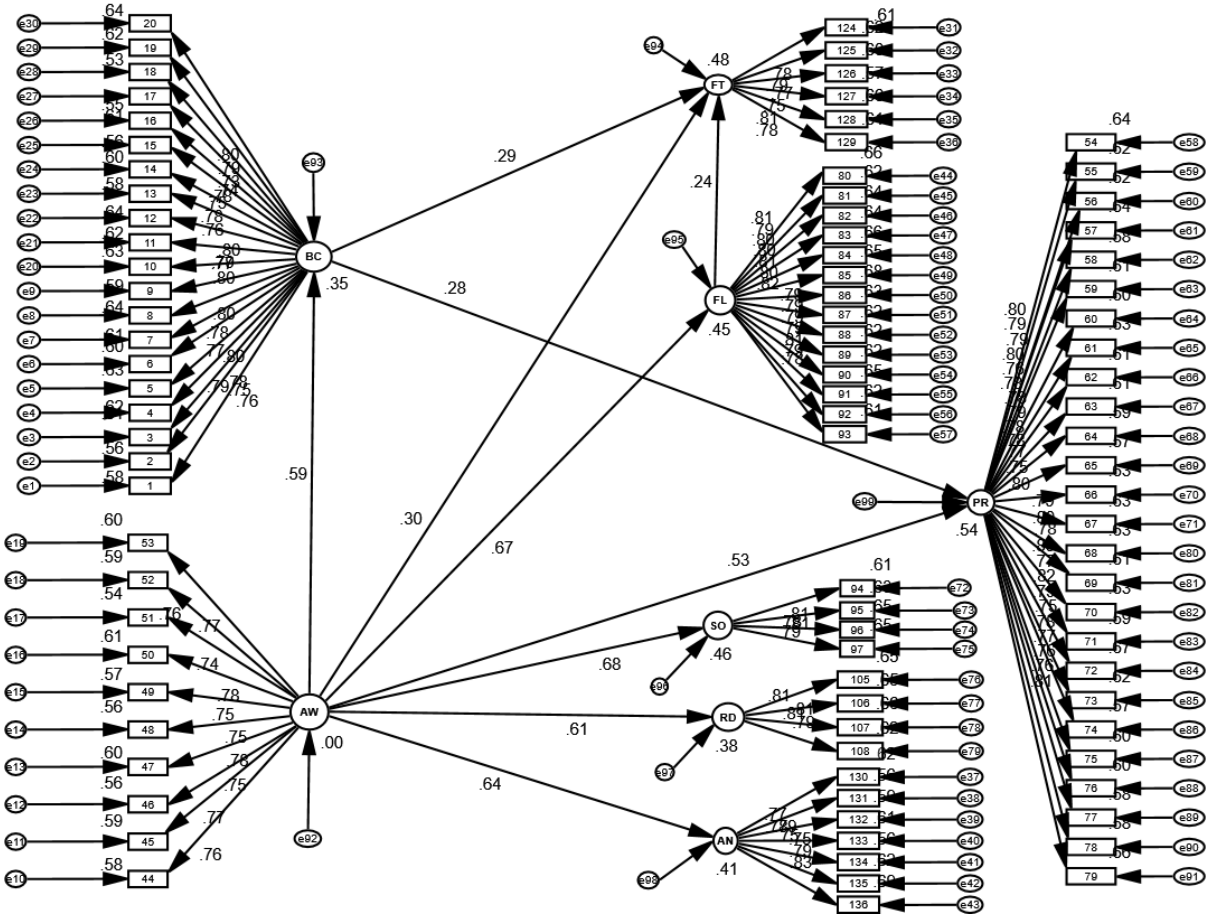


Figure 7. Final structural equation model with standardized factor loadings, standardized structural coefficients, and squared multiple correlations.

The prespecified structural equation model was estimated using maximum likelihood estimation and converged successfully. The standardized factor loadings of the 91 observed indicators ranged from 0.727 to 0.832, and all loadings were statistically significant ($p<0.001$). The chi-square test was statistically significant (χ^2 =4994.056, df =3994, $p<0.001$), with a χ^2/df ratio of 1.25. The remaining fit indices were CFI = 0.959, TLI = 0.957, IFI = 0.959, and RMSEA = 0.027, with a 90% confidence interval of 0.025–0.029. The standardized solution of the final model is presented in Figure 7. All 10 prespecified structural paths were positive and statistically significant ($p<0.001$). The standardized

effects of AW on BC, FL, SO, RD, AN, PR, and FT were 0.590, 0.668, 0.682, 0.615, 0.642, 0.532, and 0.301, respectively. The standardized effects of BC on PR and FT were 0.281 and 0.285, respectively, while the standardized effect of FL on FT was 0.239. The squared multiple correlations were 0.348 for BC, 0.446 for FL, 0.465 for SO, 0.378 for RD, 0.412 for AN, 0.539 for PR, and 0.479 for FT.

3.5. Bootstrap Validation

Bootstrap analyses were conducted using 5,000 resamples. All bootstrap samples were usable, and none were excluded because of a singular covariance matrix or failure to obtain a solution. The separate Bollen–Stine bootstrap analysis yielded a bootstrap probability of 0.223. Bias-corrected 95% bootstrap confidence intervals were calculated for the structural effects. The confidence intervals for all 10 direct paths excluded zero, with bootstrap significance values of $p<0.001$. The standardized indirect effect of AW on PR through BC was 0.166 (95% bias-corrected CI: 0.105–0.234, $p<0.001$). The total standardized indirect effect of AW on FT through BC and FL was 0.327 (95% bias-corrected CI: 0.242–0.426, $p<0.001$). The standardized total effects of AW on PR and FT were 0.698 (95% bias-corrected CI: 0.627–0.759, $p<0.001$) and 0.628 (95% bias-corrected CI: 0.545–0.699, $p<0.001$), respectively. The corresponding direct effects remained statistically significant: 0.532 for the effect of AW on PR (95% bias-corrected CI: 0.425–0.633) and 0.301 for the effect of AW on FT (95% bias-corrected CI: 0.165–0.427).

4. Discussion

The present findings indicate that resilience engineering in the investigated petrochemical complex is organized as an interdependent socio-technical system rather than as a set of independent indicators. Fuzzy DEMATEL placed management commitment, awareness, reporting culture, learning culture, teamwork, and buffering capacity predominantly on the net-influence side of the network, whereas preparedness, flexibility, self-organization, redundancy, anticipation, and fault-tolerance received more cumulative influence than they exerted. This pattern is consistent with the foundational view that resilient performance emerges through interactions among organizational, human, and technical [10,29–31]. However, the DEMATEL cause and effect terminology denotes the balance between influence dispatched and received in an expert-perceived network; it does not demonstrate temporal or experimental causation. Similarly, the cross-sectional SEM phase evaluates whether employee data are

compatible with prespecified directional relationships, but cannot exclude reciprocal effects, omitted causes, or alternative temporal sequences. The results therefore support a theoretically plausible architecture of resilience indicators rather than definitive causal laws.

The principal methodological contribution lies in the convergence of two complementary evidence sources. MMDE retained ten relationships from the expert-derived total-relation matrix before SEM estimation, and all ten prespecified paths were positive and significant in the employee sample, without adding post hoc structural paths. This convergence strengthens confidence that the retained relationships were not peculiar to one analytical method. Nevertheless, the two phases did not provide identical evidence. DEMATEL characterized overall network position and cumulative influence, whereas SEM estimated specific conditional relationships among selected constructs. Accordingly, management commitment, reporting culture, learning culture, and teamwork remained influential expert-derived indicators but were not directly tested as predictors in SEM. Conversely, flexibility was a net-effect indicator in the complete DEMATEL network but still had a significant specific effect on fault-tolerance. This distinction is central to the study: prominence, net network role, and path-specific influence describe different properties and should not be interpreted interchangeably.

The overall structure is compatible with recent process-industry literature that distinguishes organizational, human, risk-management, and technical dimensions of resilience[32–34].Management commitment, communication, reporting, and learning shape priorities, information flow, resource allocation, and the legitimacy of adaptive action; preparedness, anticipation, flexibility, redundancy, and fault-tolerance describe capacities that become visible when the system encounters increasing demand or disruption. This does not imply a rigid one-way hierarchy, because adaptive capabilities can also generate feedback and learning. It does suggest, however, that visible operational preparedness or technical reserve may not be sustainable when informational and organizational conditions are weak. Previous reviews have similarly identified management commitment, awareness, learning, and flexibility as recurrent resilience indicators, while emphasizing the need to analyze their interactions rather than treating them as isolated checklist items[32–35].

Awareness was the most consequential indicator across both phases. It exerted the greatest total influence in DEMATEL, was the source of seven MMDE-retained relationships, and showed positive

SEM associations with buffering capacity, flexibility, self-organization, redundancy, anticipation, preparedness, and fault-tolerance. The strongest standardized relationships were observed for self-organization and flexibility, whereas the direct relationship with fault-tolerance was smaller. This ordering suggests that awareness may operate primarily through organizational and cognitive capacities that coordinate adaptive performance, rather than directly replacing the material and technical requirements of fault tolerance. Earlier petrochemical research also ranked awareness, preparedness, and flexibility among the most important resilience factors[6], but the present study extends that evidence by showing that awareness occupied a predominantly dispatching position and was connected to a wider set of adaptive capabilities.

In tightly coupled process operations, awareness should be understood as a distributed capacity to obtain, communicate, and interpret safety-relevant information, not merely as individual vigilance. It may depend on accurate mental models of the process, early interpretation of deviations, quality of shift handovers, consistency between control-room and field information, and visibility of equipment, barrier, and backup-resource status. Recent work on industrial sensemaking shows that converting process deviations into contextualized information can support earlier and more appropriate operator intervention[36]. An empirical study of continuous-shift industrial work likewise demonstrated that communication during shift change is integral to distributed situation awareness[37], while a recent control-room review emphasized the centrality of human, organizational, interface, and environmental factors to safe control-room performance [38]. These studies provide a plausible explanation for the positive relationships of awareness with anticipation, preparedness, and flexibility: organizations must first recognize and interpret current conditions before they can project possible developments, mobilize resources, or select an appropriate alternative response.

The strong association between awareness and self-organization is particularly relevant in petrochemical operations. Self-organization should not be interpreted as unrestricted improvisation or removal of formal control. In a high-risk process plant, it more plausibly denotes the bounded ability of interdependent teams to redistribute attention, coordinate roles, and adjust task allocation when routine arrangements become insufficient. Such adaptation requires a sufficiently shared representation of system status, priorities, and the actions of other units. A previous integrated resilience engineering study in a petrochemical plant also treated self-organization as part of a broader, interdependent set of

resilience indicators[5] . The present results provide initial empirical support for a theoretically plausible relationship between distributed awareness and self-organization, while recognizing that the precise communication and coordination mechanisms were not measured directly.

Awareness was also related to redundancy and buffering capacity, but these constructs are not synonymous. Redundancy concerns substitute components, pathways, roles, or resources; buffering capacity concerns the margin available to absorb additional demand or disruption; and fault-tolerance concerns maintaining acceptable performance in the presence of failure. Awareness does not create spare resources, but it can influence whether vulnerabilities are recognized, whether backup resources are correctly located and maintained, and whether their availability and activation conditions are understood. This interpretation helps explain why the direct effect of awareness on fault-tolerance was smaller than its combined indirect effect through buffering capacity and flexibility. The total effect of awareness on fault-tolerance was 0.628, including a significant aggregate indirect effect of 0.327. Thus, recognizing an abnormal condition appears insufficient unless the organization also has usable operating margin and feasible adaptive alternatives. This finding is consistent with the view that resilience depends on retaining adaptive capacity near operational boundaries, while remaining complementary to equipment integrity, maintenance, protective layers, and technically fault-tolerant design[30,34,35]

Buffering capacity occupied a distinctive network position. It had high prominence and substantial dispatched influence, but its relation index was close to zero. Its importance should therefore be interpreted through extensive reciprocal involvement rather than through a categorical upstream label. Buffering capacity can support preparedness and fault-tolerance by providing time, personnel, equipment, information, and operational margin, but its development also depends on management priorities, hazard awareness, maintenance, and resource allocation. SEM strengthened this interpretation: awareness was positively related to buffering capacity, which in turn was related to preparedness and fault-tolerance. The indirect association of awareness with preparedness through buffering capacity was significant, and the total effect of awareness on preparedness reached 0.698. This pattern suggests that information becomes operational readiness when the organization possesses sufficient resources and margin to translate recognition into action. It is also consistent with the earlier

petrochemical AHP study that ranked management commitment, buffering capacity, and reporting culture as the most influential indicators [27].

Preparedness was the most prominent and the most strongly influenced indicator in DEMATEL, yet it belonged to the net-effect group. This apparent paradox demonstrates why importance and net influence must be separated. Preparedness is not a passive outcome; it is an integrative capability that depends on credible scenarios, role clarity, competence, communication, equipment availability, coordination, and mobilizable resources. Awareness and buffering capacity jointly explained more than half of its variance in SEM, supporting the interpretation that preparedness develops through an informational and resource base rather than through plans or exercises alone. The finding is consistent with earlier petrochemical evidence regarding the importance of preparedness[6], while adding a structural explanation for why a highly important indicator can still be predominantly influence-receiving.

Flexibility showed a similarly informative dual role. Although it received more influence than it exerted across the full DEMATEL network, it had a positive direct effect on fault-tolerance and contributed to the indirect association between awareness and fault-tolerance. Once established, flexibility may help maintain performance through changes in task allocation, operating configuration, resource use, or response strategy. However, this result should not be generalized as evidence that more discretion is always beneficial. Research in another high-risk setting shows that resilience depends on balancing flexibility with coordination, rules, and control, and that both excessive rigidity and poorly governed adaptation can undermine safety[39]. The present findings therefore support informed and bounded flexibility based on reliable awareness, competence, authorization, and intact process-safety barriers.

management commitment had the largest positive relation index but lower prominence than several operational indicators, suggesting an upstream leverage role rather than dense direct involvement in every relationship. Senior management can influence staffing, maintenance priorities, training, reserve resources, reporting legitimacy, and the authority to suspend or modify work. This interpretation is supported by the petrochemical AHP results[27] and by a management-level study in which reporting safety issues was central across levels, middle and lower managers emphasized management commitment, and senior managers emphasized flexibility[40]. Reporting and learning cultures can be understood as complementary components of the same informational cycle: reporting makes

deviations, near misses, degraded barriers, and successful adaptations visible, while learning converts those observations into revised knowledge, training, procedures, or design. A recent scoping review similarly conceptualized learning from resilient performance as understanding the system, sharing knowledge, and redesigning system properties[41]. Teamwork may enable these processes to cross organizational boundaries, although its specific pathways require future SEM testing because it was not retained as a direct predictor in the present structural model.

Differences between the present findings and previous rankings should not be treated automatically as inconsistency. Fuzzy cognitive mapping identified awareness, preparedness, and flexibility as the most important factors [6]; AHP and TOPSIS prioritized management commitment, buffering capacity, and reporting culture [27]; and integrated resilience studies demonstrated the value of adding teamwork, self-organization, redundancy, and fault-tolerance [5]. These approaches answer different questions. Priority methods estimate relative importance, whereas DEMATEL distinguishes total involvement from the balance of influence dispatched and received. SEM then estimates conditional relationships within a restricted model. Differences may also reflect plant technology, safety maturity, resource constraints, centralization, recent incident experience, and expert composition. The present study therefore complements rather than replaces earlier assessments by clarifying why a highly important capability may be a net receiver and why a net-effect indicator may still exert a meaningful specific influence.

The study has practical implications, but their interpretation requires restraint. The results suggest that resilience programs should not focus only on downstream outputs such as completed emergency plans, backup-equipment counts, or perceived fault-tolerance. Improving shift handovers, integrating control-room and field information, making critical barrier and backup-resource status visible, providing feedback on deviation and near-miss reports, and examining successful adaptations may strengthen the informational conditions from which preparedness and flexible response emerge[36–38,41]. Mapping actual rather than nominal resource margins may similarly improve buffering capacity. These are evidence-informed intervention priorities, not interventions whose effectiveness was tested here, and they should supplement rather than replace conventional process safety management, maintenance, and barrier control.

5. Conclusion

This study developed and empirically evaluated an integrated structural model of resilience engineering indicators in the petrochemical industry using fuzzy DEMATEL, MMDE, and structural equation modeling. The findings indicate that resilience is shaped through an interdependent configuration of managerial, informational, cultural, and operational indicators rather than through isolated organizational attributes. In the expert-derived network, management commitment, awareness, reporting culture, learning culture, teamwork, and buffering capacity predominantly occupied upstream positions, whereas preparedness, flexibility, self-organization, redundancy, anticipation, and fault-tolerance were more dependent on the broader system structure.

Awareness emerged as the most influential upstream indicator and was positively associated with several adaptive indicators, particularly self-organization, flexibility, anticipation, preparedness, and redundancy. Its weaker direct relationship with fault-tolerance, together with the significant indirect associations through buffering capacity and flexibility, indicates that the contribution of awareness may depend partly on its translation into usable resources, operational margins, and feasible response alternatives. Preparedness and flexibility also showed that indicators receiving substantial influence within the overall network may still exert meaningful effects along specific structural paths.

The principal contribution of the study lies in integrating expert-derived influence mapping with employee-based structural testing. This approach distinguishes overall prominence, net network position, and path-specific influence as related but non-interchangeable properties. The findings support the prioritization of awareness, management commitment, reporting, learning, teamwork, and buffering capacity as potential enabling indicators, while preparedness, flexibility, and fault-tolerance may serve as operational indicators of how effectively these enabling conditions are translated into adaptive performance. These priorities should complement established process-safety controls, technical reliability measures, and barrier-management practices.

Limitations and Future Perspectives

The findings should be interpreted in light of the expert-judgment basis of the fuzzy DEMATEL analysis and the cross-sectional, self-reported data collected from employees of a single petrochemical complex. These characteristics limit the generalizability of the findings and preclude definitive conclusions regarding temporal ordering and causality. Future studies should examine the identified relationships using longitudinal designs, objective performance indicators, and multicenter samples.

Conflict of Interest

The authors declare that they have no known financial or personal conflicts of interest that could have influenced the work reported in this study.

Funding

This study received no specific funding.

Acknowledgment

The authors gratefully acknowledge all experts and participants who generously contributed their time and expertise to this study. The authors also thank those who assisted with the coordination of data collection and study implementation.

CRediT authorship contribution statement

R.Y: Methodology, Formal analysis, Investigation, Data curation, Writing – original draft. **F.G:** Conceptualization, Supervision, Validation, Writing – review & editing. **A.A:** Methodology, Formal analysis, Software, Writing – original draft. **G.A.S:** Conceptualization, Supervision, Project administration, Writing – review & editing. **P.R:** Conceptualization, Writing – original draft, Writing – review & editing, Visualization.

Ethics Approval Declaration

This study was reviewed and approved by the Ethics Committee of Abadan University of Medical Sciences (Approval Code: IR.ABADANUMS.REC.1403.096).

Data Availability Statement

The data supporting the findings of this study are available from the corresponding author upon reasonable request. The dataset is not publicly available because of institutional confidentiality requirements and ethical considerations related to participant privacy.

References

1. Cheng, C. W., Yao, H. Q. & Wu, T. C. Applying data mining techniques to analyze the causes of major occupational accidents in the petrochemical industry. *J. Loss Prev. Process Ind.* **26**, 1269–1278 (2013).

2. Wu, Q. *et al.* Pro-growth giant business, lock in, sustainable urban development and effect on local political economy: The case of petrochemical industry at Nanjing. *J. Clean. Prod.* **107**, 324–332 (2015).

3. Abech, M. P., Berg, G. A., Delis, M. G., Guimarães, L. B. M. & Woods, D. D. Analyzing resilience of an oil distribution plant. in *Proceedings of the 2006 IEEE Systems and Information Engineering Design Symposium, SIEDS'06* 216–221 (2006). doi:10.1109/SIEDS.2006.278679.

4. Shirali, G. A., Motamedzade, M., Mohammadfam, I., Ebrahimipour, V. & Moghimbeigi, A. Challenges in building resilience engineering (RE) and adaptive capacity: A field study in a chemical plant. *Process Saf. Environ. Prot.* **90**, 83–90 (2012).

5. Azadeh, A., Salehi, V., Ashjari, B. & Saberi, M. Performance evaluation of integrated resilience engineering factors by data envelopment analysis: The case of a petrochemical plant. *Process Saf. Environ. Prot.* **92**, 231–241 (2014).

6. Azadeh, A., Salehi, Arvan & Dolatkhah, M. Assessment of resilience engineering factors in high-risk environments by fuzzy cognitive maps: A petrochemical plant. *Saf. Sci.* **68**, 99–107 (2014).

7. Nemeth, C. P. Resilience Engineering : The Birth of a Notion. in *Resilience Engineering Perspectives, Volume 1* 3–10 (2008).

8. Shirali, G. A., Mohammadfam, I. & Ebrahimipour, V. A new method for quantitative assessment of resilience engineering by PCA and NT approach: A case study in a process industry. *Reliab. Eng. Syst. Saf.* **119**, 88–94 (2013).

9. Heikkil, J. *et al. Proactive and Flexible Safety Management – Resilience In*. (net, WOS, 2010).

10. Hollnagel, E., Pariès, J., Woods, D. & Wreathall, J. *Resilience Engineering in Practice: A Guidebook*. *Resilience Engineering in Practice: A Guidebook* (2011).

11. Woods, D. D. Escaping failures of foresight. *Saf. Sci.* **47**, 498–501 (2009).

12. Jain, P., Mentzer, R. & Mannan, M. S. Resilience metrics for improved process-risk decision making: Survey, analysis and application. *Saf. Sci.* **108**, 13–28 (2018).

13. Shirali, G. A. *et al.* Job stress and resilience in Iranian nurses during the COVID-19 pandemic: A case-control study. *Work* **70**, 1011–1020 (2021).

14. Rashnoudi, P., Soltani, E., Mohammadinejad, A. & Mahabadi, H. A. Investigating the impact of situational awareness and resilience on occupational stress: a case study of nurses in medical and educational hospitals in Ahvaz. *Sci. Rep.* **15**, (2025).

15. Niskanen, T. A Resilience Engineering -related approach applying a taxonomy analysis to a survey examining the prevention of risks. *Saf. Sci.* **101**, 108–120 (2018).

16. Pashapour, S., Bozorgi-Amiri, A., Azadeh, A., Ghaderi, S. F. & Keramati, A. Performance optimization of organizations considering economic resilience factors under uncertainty: A case study of a petrochemical plant. *J. Clean. Prod.* **231**, 1526–1541 (2019).

17. Dormady, N., Roa-Henriquez, A. & Rose, A. Economic resilience of the firm: A production theory approach. *Int. J. Prod. Econ.* **208**, 446–460 (2019).

18. Sahebjamnia, N., Torabi, S. A. & Mansouri, S. A. Building organizational resilience in the face of multiple disruptions. *Int. J. Prod. Econ.* **197**, 63–83 (2018).

19. Yousefzadeh, S. *et al.* Comparative analysis of hydrometallurgical methods for the recovery of Cu from circuit boards: Optimization using response surface and selection of the best technique by two-step fuzzy AHP-TOPSIS method. *J. Clean. Prod.* 119401 (2019) doi:10.1016/j.jclepro.2019.119401.

20. Ramya, S. & Devadas, V. Integration of GIS, AHP and TOPSIS in evaluating suitable locations for industrial development: A case of Tehri Garhwal district, Uttarakhand, India. *J. Clean. Prod.* **238**, 117872 (2019).

21. Azimifard, A., Moosavirad, S. H. & Ariafar, S. Selecting sustainable supplier countries for Iran's steel industry at three levels by using AHP and TOPSIS methods. *Resour. Policy* **57**, 30–44 (2018).

22. Liu, W., Hu, Y. & Huang, Q. Research on Critical Factors Influencing Organizational Resilience of Major Transportation Infrastructure Projects: A Hybrid Fuzzy DEMATEL-ISM-MICMAC Approach. *Buildings* **14**, 1598 (2024).

23. Yeganeh, R., Mohammadfam, I., Soltanian, A. & Mirzaei Aliabadi, M. An integrative fuzzy Delphi decision-making trial and evaluation laboratory (DEMATEL) study on the risk perception-influencing factors. *Int. J. Occup. Saf. Ergon.* **29**, 1135–1146 (2023).

24. Rajabi, F., Mokarami, H., Cousins, R. & Jahangiri, M. Structural equation modeling of safety performance based on personality traits, job and organizational-related factors. *Int. J. Occup. Saf. Ergon.* **28**, 644–658 (2022).

25. Wolf, E. J., Harrington, K. M., Clark, S. L. & Miller, M. W. Sample Size Requirements for Structural Equation Models: An Evaluation of Power, Bias, and Solution Propriety. *Educ. Psychol. Meas.* **73**, 913–934 (2013).

26. Li, C.-W. & Tzeng, G.-H. Identification of a threshold value for the DEMATEL method using the maximum mean de-entropy algorithm to find critical services provided by a semiconductor intellectual property mall. *Expert Syst. Appl.* **36**, 9891–9898 (2009).

27. Shirali, G. A., Rashnoudi, P., Salehi, V. & Ghanbari, S. A hierarchical assessment of resilience engineering indicators in petrochemical industries using AHP and TOPSIS. *Hum. Factors Ergon. Manuf.* **33**, 3–26 (2023).

28. Soltani, E., Mohammadinejad, A., Rashnoudi, P. & Ahmadi, O. A fuzzy based hybrid approach

for risk assessment of anesthesiologists using OPA and EDAS methods. *Sci. Rep.* **15**, 1–16 (2025).

29. Wears, R. L. Resilience Engineering: Concepts and Precepts. *Qual. Saf. Heal. Care* **15**, 447–448 (2006).

30. Woods, D. D. Four concepts for resilience and the implications for the future of resilience engineering. *Reliab. Eng. Syst. Saf.* **141**, 5–9 (2015).

31. Righi, A. W., Saurin, T. A. & Wachs, P. A systematic literature review of resilience engineering: Research areas and a research agenda proposal. *Reliab. Eng. Syst. Saf.* **141**, 142–152 (2015).

32. Ranasinghe, U., Jefferies, M., Davis, P. & Pillay, M. Resilience Engineering Indicators and Safety Management: A Systematic Review. *Saf. Health Work* **11**, 127 (2020).

33. Ghaljahi, M., Omidi, L. & Karimi, A. Resilience assessment in process industries: A review of literature. *Heliyon* **11**, e42498 (2025).

34. Emkani, M., Alimohammadlou, M., Zarei, E., Jahangiri, M. & Kamalinia, M. A quantitative multi-dimensional resilience framework in process industries. *Eng. Appl. Artif. Intell.* **161**, 112100 (2025).

35. Valente, M., Ricci, F. & Cozzani, V. A systematic review of Resilience Engineering applications to Natech accidents in the chemical and process industry. *Reliability Engineering and System Safety* vol. 255 at https://doi.org/10.1016/j.ress.2024.110670 (2025).

36. Bakhshandeh, M., Liyanage, J. P., Andre Asheim, B. & Li, L. Process deviations, early sensemaking, and enabling operators: thinking beyond the traditional alarm-based practice to enhance industrial resilience. *ElsevierM Bakhshandeh, JP Liyanage, BA Asheim, L LiJournal Saf. Sustain. 2024•Elsevier* **1**, 161–172 (2024).

37. Rosário, C. R., Amaral, F. G., Kuffel, F. J. M., Kipper, L. M. & Frozza, R. Using Bayesian belief networks to improve distributed situation awareness in shift changeovers: A case study. *Expert*

Syst. Appl. **188**, 116039 (2022).

38. Janizadeh, R., Choobineh, A., Charkhabi, S. A. & Jahangiri, M. Looking beyond the screen: A systematic review of safety in control rooms. *Heliyon* **10**, e25118 (2024).

39. Jubault Krasnopevtseva, N., Thomas, C. & Kaminska, R. Organizing for resilience in high-risk organizations: The interplay between managerial coordination and control in resolving stability/flexibility tensions in a nuclear power plant. *J. Bus. Res.* **189**, (2025).

40. Salehi, V. & Veitch, B. Measuring and analyzing adaptive capacity at management levels of resilient systems. *J. Loss Prev. Process Ind.* **63**, 104001 (2020).

41. Degerman, H. & Wallo, A. Conceptualising learning from resilient performance: A scoping literature review. *Appl. Ergon.* **115**, 104165 (2024).

42. Cooper, B. *et al.* Addressing common method variance and endogeneity in vocational behavior research: A review of the literature and suggestions for future research. *J. Vocat. Behav.* **121**, 103472 (2020).